Journal of Applied Mechanics and Technical Physics, Vol. 51, No. 2, pp. 280–287, 2010

PLASTICITY MODEL FOR METALS UNDER CYCLIC LARGE-STRAIN LOADING

V. M. Greshnov and I. V. Puchkova

UDC 539.3; 621.735.043

This paper deals with mathematical modeling of one of the effective technologies of plastic metal forming — multistep cold metal forging. Experimental results are given on the plastic behavior of metals under cyclic loading at large strains accumulated for one cycle. Based on the experimental data obtained, a plasticity model is developed and shown to be effective in testing and improving the technology of forging a nut blank by using a computer-aided engineering analysis system.

Key words: *plasticity, cyclic deformation, plastic metal working, computer system of the engineering analysis.*

Introduction. The effectiveness of using computer-aided engineering analysis systems in mechanical engineering is widely recognized. One trend in the development of such systems is to improve the models used to describe material properties. The cold die forging technology is an advanced technology of modern mechanical engineering [1]. It produces 50–300 articles for 1 min (for example, bolts, nuts, rivets, etc.) at an average metal recovery equal to 95%.

Plastic working of parts of complex geometrical shapes is performed in 3–5 processing steps involving complex loading and nonmonotonic (frequently cyclic) deformations. The accumulated strains reach 1–4 units [2], and in each step, the strain is 0.4–0.8. Cold deformation of metals leads to deformation anisotropy of mechanical properties; i.e., it is accompanied by isotropic and kinematic hardening [3].

The above-mentioned features of plastic deformation involved in cold volumetric forging are responsible for difficulties in its mathematical modeling. The classical plasticity models used in the computation kernels of the ANSYS, DEFORM, Q-FORM, etc., software products do not describe this deformation, and the technology is therefore developed on the basis of the production experience with all disadvantages inherent in this method.

In recent decades, a large number of plasticity models (see [4–6]) have been proposed to take into account loading history and kinematic hardening. An analysis of these models is beyond the scope of the present paper. We only note that the main idea underlying these models is to refine the evolution equation for the additional stress treated as an internal parameter which was introduced in 1956 by A. Yu. Ishlinskii and V. Prager. This stress describes deformation anisotropy [3]. These models were designed to develop methods for the strength and creep calculation of machine components and were therefore tested in experiments with strains not exceeding 2–4%. There have been almost no attempts to study cyclic deformation at large strains accumulated for one cycle, as is the case in plastic metal working.

This paper presents experimental data and a new approach to the development of a plasticity model for describing cold deformation of metals at large and alternating strains.

1. Experimental Technique and Results. The objective of this work was to experimentally study the plastic behavior of metals under cyclic deformation with large strains accumulated for one and several cycles. The samples having the shape of a rectangular parallelepiped with dimensions $66 \times 40 \times 12$ mm were made of preliminarily annealed (isotropic) high-quality 10kp grade steel. Deformation of the samples was performed on a hydraulic ram in a special device (Fig. 1) made of die steel and subjected to thermal processing — quenching and tempering. The sample was coated with a lubricant (suspension of flaky graphite in mineral oil) and was deformed

Ufa State Aviation Technical University, Ufa 450000; Greshnov_VM@list.ru. Translated from Prikladnaya Mekhanika i Tekhnicheskaya Fizika, Vol. 51, No. 2, pp. 160–169, March–April, 2010. Original article submitted April 15, 2009.

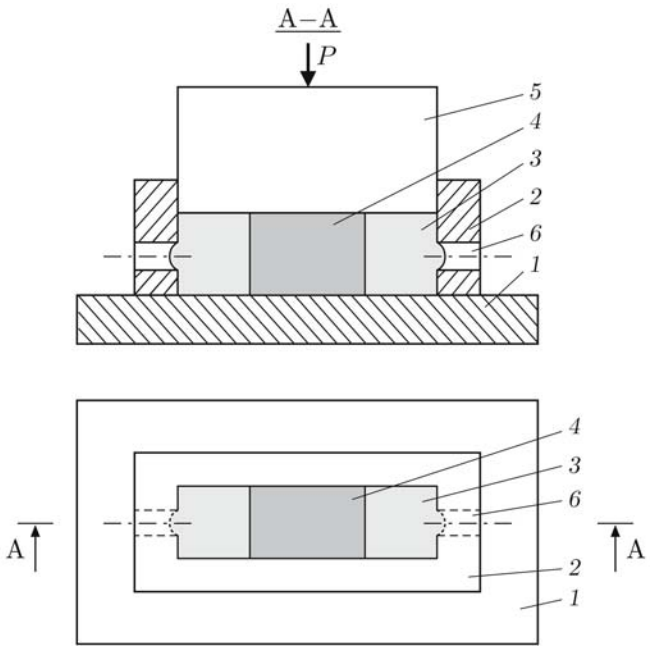

Fig. 1. Setup for deformation of samples: 1) support plate; 2) die; 3) disposable insert; 4) sample; 5) punch; 6) hole through which the insert material is extruded.

at room temperature in the device (upset under plane deformation) by a punch. Disposable inserts made of lead were placed on both sides of the sample in the device to ensure high plasticity of steel. During deformation, lead was extruded through the die holes, which provided high hydrostatic pressure and steel plasticity sufficient for the experiment. After the first upsetting, the sample, together with the lead inserts, was pressed out from the die by the punch, cleaned, if necessary, placed in the device, and rotated by 90° relative to the initial position; after that, the lead inserts were replaced and the sample was subjected to repeated deformation. One operation cycle included triple deformation of the sample. The strain intensity accumulated for one cycle was equal to unity. The working of the other two samples included, respectively, two and three cycles described above. The samples were cut along the largest dimension into three identical pieces, which were used to produce two standard cylindrical samples for tension tests and three cylindrical samples for compression tests. During standard tests of the samples, the yield points were determined, which were compared with the plastic strain intensity accumulated by the sample.

The results of the experimental study were used to plot curves of stress intensity versus strain intensity $\sigma(\varepsilon)$ (Fig. 2).

According to another technique, cylindrical samples 15 mm in diameter and 80 mm long made of M1 copper and AD1 aluminum were subjected to cyclic deformation under the hourglass forming scheme. The results obtained using this technique are taken from [7]. In one working cycle, the average strain of the sample was 0.57. By varying the number of cycles, samples with various accumulated plastic strain intensities were obtained. Deformation of the samples ended with direct extrusion. The resulting bars were used to produce standard samples for tension and upsetting tests. As in the first technique, conditional yield points were determined, which were put in correspondence to the plastic strain intensity accumulated by the sample. For the purpose of averaging experimental results, three samples were subjected to deformation in each mode.

The obtained dependences of the stress intensity σ on the plastic strain intensity ε are given in Fig. 3. The vertical segments in Figs. 2 and 3 show the symmetric 10% deviation from the average value of σ.

In addition, the dependences $\sigma(\varepsilon)$ and $\sigma = \Phi(\varepsilon)$ (curves 1 and 2 in Figs. 2 and 3) for 10kp steel, M1 copper, and AD1 aluminum were calculated for monotonic deformation according to the equation of the isotropic plasticity model [8]

$$\sigma = \beta m G b \Big(\frac{(b\lambda)^{-1}[\exp(\varepsilon) - 1] + \rho_{s0}}{\exp(\varepsilon)} \Big)^{1/2} \tag{1}$$

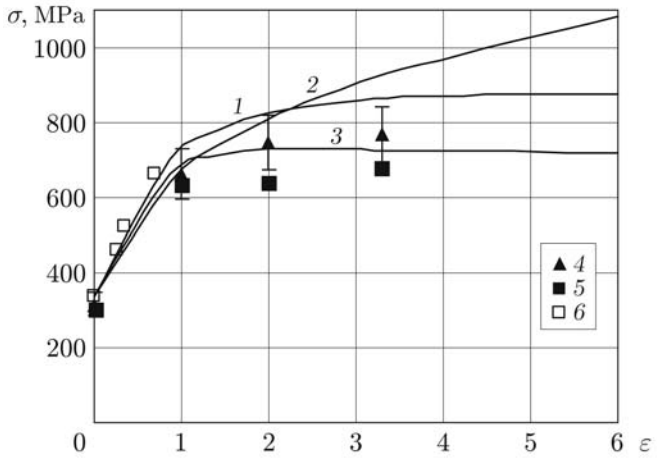

Fig. 2. Experimental (points) and calculated (curves) dependences of stress intensity on strain intensity for 10kp grade steel: 1) calculation using formula (1); 2) calculation using formula (3); 3) calculation using formula (7); 4) tension test; 5) compression test; 6) monotonic compression test.

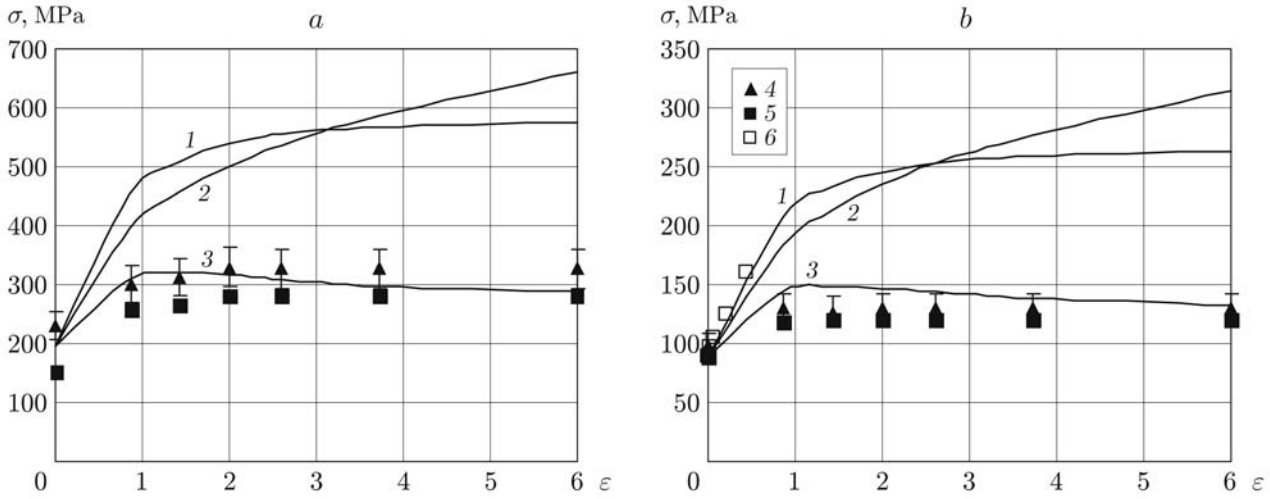

Fig. 3. Experimental (points) and calculated (curves) dependences of stress intensity on strain intensity: (a) M1 copper; (b) AD1 aluminum (notation the same as in Fig. 2).

and the equation of the plasticity model of an isotropic material with isotropic-kinematic hardening [2]

$$\Phi(\varepsilon) = \frac{\beta m G b}{2}\Big[\Big(\frac{(b\lambda)^{-1}[\exp(\varepsilon)-1]+\rho_{s0}}{\exp(\varepsilon)}\Big)^{1/2} + (\rho_{s0}+A\varepsilon)^{1/2}\Big]. \tag{2}$$

Here $\beta = 0.4$ is a coefficient, $m = 3.1$ is the Taylor factor for polycrystals, $b = 3\cdot 10^{-8}$ cm is the dislocation Burgers vector modulus, ρ_{s0} is the initial scalar dislocation density in the material, λ is the mean dislocation free path, and A is a coefficient determined experimentally.

Different sample materials and deformation schemes were chosen to determine the reliability of the regularities found.

The most important result obtained in the study is the finding that the stress intensity during cyclic (complex) deformation was much lower than that during monotonic deformation (see Figs. 2 and 3). In this case, this effect is more pronounced (especially for nonferrous metals) than in the case of small strains [4–6]. For copper and aluminum, the value of σ decreases by 46% compared to the value of σ in the case of monotonic deformation (see Fig. 3). The physical meaning of this effect was discussed in [3].

In both cyclic and monotonic deformation, stabilization of the process (σ = const) was observed. In the first case, this occurs at accumulated strain intensity ε = 1–2, and in the second, at ε = 2–3 (see Figs. 2 and 3). Beginning at these strains, the material behavior is described with high accuracy by the ideal plastic model.

During cyclic deformation of metals in the case of large strains, insignificant anisotropy of the flow stress (point in Figs. 2 and 3) arises and remains constant. The ratio of the difference between the values of σ for tension and compression to the average value of σ for various values of ε does not exceed 16% for copper and aluminum and 11% for steel. These values correspond to the well-known scatter of strength characteristics of structural metals and alloys determined by standard methods.

In the plasticity theory of isotropic materials with isotropic-kinematic hardening [2], the stress function (2) more accurately describes the plastic behavior of metals under complex loading for accumulated strain intensities not exceeding ε = 0.5–0.7 (in the case of steel, $\varepsilon \leqslant 2$) (curves 2 in Figs. 2 and 3) compared to the isotropic model (1). From the results presented in Figs. 2 and 3 (curves 2), it follows that at $\varepsilon > 1$ for M1 copper and AD1 aluminum and at $\varepsilon > 2$ for steel, according to (2), there is continuous hardening and an increase in the difference between the theoretical and experimental dependences $\Phi(\varepsilon)$.

2. Plasticity Model for Cyclic Deformation. An analysis of the experimental results given above shows that, in the first deformation cycles, the initial plasticity surface of the material $f(\sigma_{ij}, \sigma_{\text{yield}}, \varepsilon) = 0$ in the stress space is slightly displaced as a whole with simultaneous isotropic expansion. For ε = 1, there is stabilization of the stress (σ = const). During the further deformation, the shape of the plasticity surface does not vary. Therefore, in the plasticity model, kinematic hardening can be ignored (because of its smallness) and only isotropic hardening in the range $\varepsilon \in [0, 1]$ should be taken into account. Hence, we can write isotropic governing relations similar to the relations of flow theory for an isotropic material [3]:

$$d\varepsilon_{ij} = \frac{3}{2}\,\frac{d\varepsilon}{\Phi'(\varepsilon)}\,s_{ij}. \tag{3}$$

Here $d\varepsilon_{ij}$ is the plastic strain increment tensor (the incompressibility condition $d\varepsilon_{ii} = 0$ is adopted), $d\varepsilon$ is the plastic strain increment rate, $\Phi'(\varepsilon)$ is the stress function for cyclic large-strain deformation, and s_{ij} is the stress deviator.

Taking into account the results obtained in Sec. 1, we adopt the following hypothesis, which is in some sense similar to the single-curve hypothesis. In cyclic and similar (complex loading along polygonal paths) deformations of metals characterized by large plastic-strain intensities in the half-cycle ($\varepsilon > 0.1$–0.2) and accumulated strains $\int d\varepsilon > 1$–2, the flow stress intensity is a function of the accumulated plastic strain intensity (Odqvist parameter) which does not depend on the cycle characteristics (amplitude, symmetry, etc.) and the type of stress state. According to this hypothesis, the stress function $\Phi'(\varepsilon)$ in (3) can be taken to be the dependence $\sigma(\varepsilon)$ averaged over the results of tension and compression tests (see Figs. 2 and 3).

To obtain an analytical description of the dependences $\sigma(\varepsilon) \equiv \Phi'(\varepsilon)$, we consider the physical-phenomenological plasticity model taking into account the Bauschinger effect [9]:

$$\sigma = \beta m G b\Big(\frac{\exp(\varepsilon) - 1}{\lambda' b \exp(\varepsilon)} + \frac{\rho_{s0} + A\varepsilon^{+}}{\exp(\varepsilon)}\Big)^{1/2}. \tag{4}$$

Here σ and ε are the stress and strain for reverse deformation after forward deformation in which the strain ε^{+} is reached, and λ' is the dislocation free path after the change in the sign of deformation.

To determine the coefficients A and λ', it is recommended to perform a series of tests that includes deformation of a cylindrical sample by simple tension (drawing or direct extrusion) with strain $\varepsilon^{+} = 0.43$–0.60; cutting the resulting bar into three standard samples (for averaging results) for upsetting tests; upsetting tests of the samples and construction of a strain diagram $\sigma(\varepsilon)$. The values of A and λ' are determined from the obtained diagram $\sigma(\varepsilon)$ using the formulas

$$A = [(\sigma_{02}^{\exp})^2(\beta m G b)^{-2} - \rho_{s0}]/\varepsilon^{+}; \tag{5}$$

$$\lambda' = \frac{b(\beta m G)^2[\exp(\varepsilon) - 1]}{\sigma^2 \exp(\varepsilon) - (\beta m G b)^2(\rho_{s0} + A\varepsilon^{+})}, \tag{6}$$

where $\sigma_{02}^{\exp}$ are experimentally determined yield point of the material in compression; $\varepsilon \in (0.3; 0.5)$.

Equations (5) and (6) are obtained from (4); Eq. (5) being obtained for $\varepsilon = 0$ ($\sigma = \sigma_{02}^{\exp}$).

The scalar equation describing plastic deformation of metals under the cyclic deformation conditions studied is obtained from the model taking into account the Bauschinger effect (4) by replacing ε^+ by the current value of ε:

$$\Phi'(\varepsilon) \equiv \sigma = \beta m G b \Big(\frac{(\lambda' b)^{-1} [\exp(\varepsilon) - 1] + \rho_{s0} + A\varepsilon}{\exp(\varepsilon)} \Big)^{1/2}. \tag{7}$$

To validate the model (7), we performed calculations for 10kp steel, M1 copper, and AD1 aluminum (curves 3 in Figs. 2 and 3). From Figs. 2 and 3, it follows that the theoretical and experimental dependences are in satisfactory agreement.

The calculations were performed for the following values of material parameters: for 10kp steel, $G = 78{,}000$ MPa, $\lambda = 3.6 \cdot 10^{-4}$ cm, $\rho_{s0} = 1.3 \cdot 10^{10}$ cm^{-2}, $A = 3.1 \cdot 10^{10}$ cm^{-2}, and $\lambda' = 5.4 \cdot 10^{-4}$ cm; for M1 copper, $G = 46{,}000$ MPa, $\lambda = 2.96 \cdot 10^{-4}$ cm, $\rho_{s0} = 1.3 \cdot 10^{10}$ cm^{-2}, $A = 3.0 \cdot 10^{10}$ cm^{-2}, and $\lambda' = 1.18 \cdot 10^{-3}$ cm; for AD1 aluminum, $G = 26{,}000$ MPa, $\lambda = 4.53 \cdot 10^{-4}$ cm, $\rho_{s0} = 8.35 \cdot 10^{9}$ cm^{-2}, $A = 2.27 \cdot 10^{10}$ cm^{-2}, and $\lambda' = 1.81 \cdot 10^{-3}$ cm.

An analysis of the calculated curves 3 in Figs. 2 and 3 shows that, in some cases, Eq. (7) describes diagrams $\Phi'(\varepsilon)$ with softening (descending diagrams), i.e., for $\varepsilon > 1$ and $d\Phi'/d\varepsilon < 0$. Use of this diagram can involve some difficulties in determining the stress–strain state of blanks during plastic metal working. As noted above, for $\varepsilon > 1$, the plastic behavior of materials is described by the ideal plastic model with accuracy admissible for design calculations. Therefore, in the formulation and solution of boundary-value plasticity problems, it seems reasonable to use the governing relations (3) and (7) for the first deformation step involving hardening (see Figs. 2 and 3), and for the second step ($\Phi' = \text{const}$), it is expedient to use the boundary-value problem formulated using ideal plasticity theory with the plasticity condition

$$((3/2) s_{ij} s_{ij})^{1/2} = \sigma'_{\text{yield}} \tag{8}$$

[$\sigma'_{\text{yield}} = \Phi'(\varepsilon) = \text{const}$] and the governing relations [3]

$$d\varepsilon_{ij} = \frac{3}{2} \frac{d\varepsilon}{\sigma'_{\text{yield}}} s_{ij}. \tag{9}$$

The duration of the first step and the value of σ'_{yield} are determined from the dependence $\Phi'(\varepsilon)$ constructed for the material studied by Eq. (7).

Thus, according to the hypothesis formulated above, the behavior of metals under cyclic deformation with large strains in half-cycles and with strains accumulated for several cycles in the coordinates "stress intensity–accumulated strain intensity" can correspond to the behavior of some abstract isotropic material under simple loading and monotonic deformation, whose strain diagram $\Phi'(\varepsilon)$ is determined taking into account some cyclic deformation parameters of real metals.

As is known, the equations of flow theory (3) and ideal plasticity theory (8), (9) provide satisfactory results in the determination of the stress–strain state of blanks under plastic metal working involving simple loading and monotonic deformation. Equation (7) adequately describes experimental dependences $\sigma(\varepsilon)$ (curves 3 in Figs. 2 and 3), and this dependence is therefore sufficient for mathematical modeling of technological processes of plastic metal working.

3. Improving the Technology of Forging a Nut Blank. The forging of a nut blank of 38KhGNM steel includes five operations. The nut forging technology was tested by mathematical modeling using the plasticity model developed.

According to the technology of preparing material for cold forging, high-quality steels, including steel 38KhGNM, are subjected to spheroidizing annealing to increase plasticity and reduce strain resistance. Therefore, in the initial state, steel is isotropic.

According to the technique described in Sec. 2, experimental strain diagrams are constructed (Fig. 4) and parameters of the model are determined: $G = 81\,410$ MPa, $\rho_{s0} = 2.8 \cdot 10^{10}$ cm^{-2}, $\lambda = 2.1 \cdot 10^{-4}$ cm, $\beta = 0.4$, $m = 3.1$, $b = 3 \cdot 10^{-8}$ cm, $\varepsilon^+ = 0.51$, $A = 5.594 \cdot 10^{10}$ cm^{-2}, and $\lambda' = 2.18 \cdot 10^{-4}$ cm.

The dependence $\Phi'(\varepsilon)$ calculated by Eq. (7) for 38KhGNM steel (Fig. 5) and Eq. (3) were used to calculate some stress–strain characteristics of the blank in forging steps using the computer-aided engineering (CAE) DEFORM-3D software.

Because of the symmetry of the blank, the boundary-value problem of determining the stress–strain characteristics of the blank in the forging steps was posed in the axisymmetric formulation. The system of equations

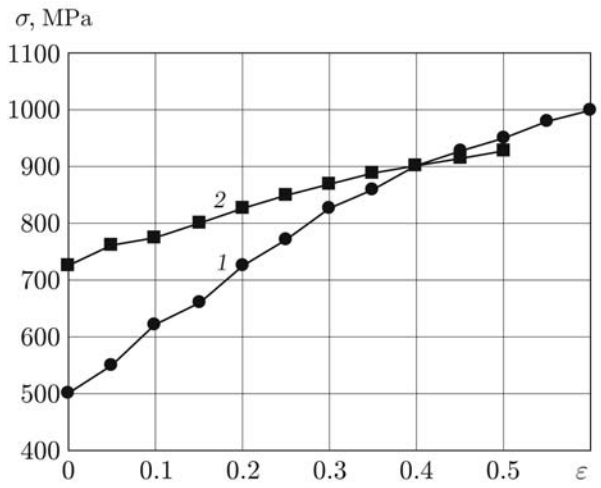

Fig. 4

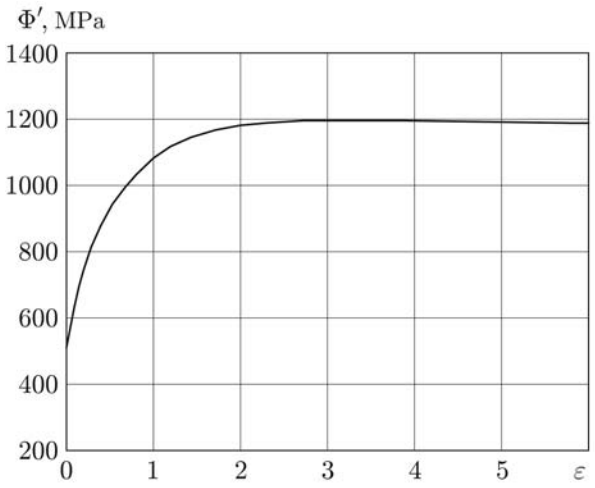

Fig. 5

Fig. 4. Experimental strain diagrams for 38KhGMN steel: 1) initial state; 2) upsetting after preliminary deformation by simple tension for $\varepsilon^{+} = 0.51$ (bar drawing).

Fig. 5. Dependence $\Phi'(\varepsilon)$ for 38KhGMN steel.

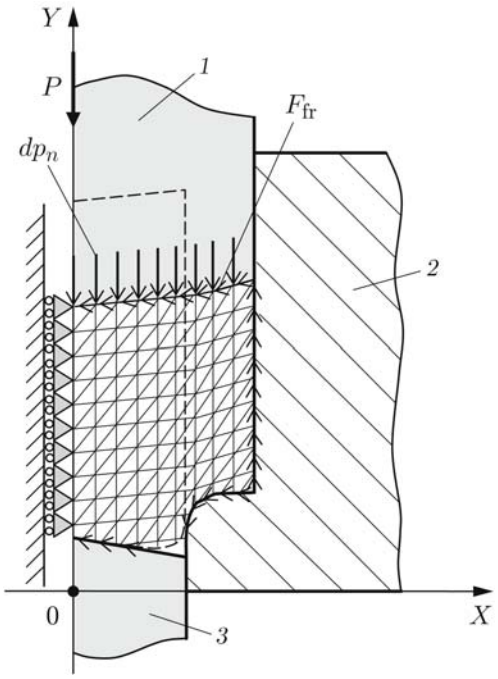

Fig. 6. Computation finite-element scheme for deformation of the blank in the second step of forging: 1) punch; 2) die; 3) extruder.

consists of differential equilibrium equations, the Cauchy kinematic relations [2, 3] and the governing relations (3) and (7). As an example Fig. 6 shows the computation deformation scheme at the end of forming of the blank in the second forging step, which is typical of other steps. Because the problem is axisymmetric, the stress–strain characteristics were determined in 1/2 meridional sections of the blank.

In the first step, the cylindrical blank cut from the bar is calibrated, after which the blank is placed in the cavity of the die block formed by the die, extruder, and punch for the second step (shown by a dashed line in Fig. 6). The punch moves downward and deforms the blank; as a result, the blank fills the cavity of the die block.

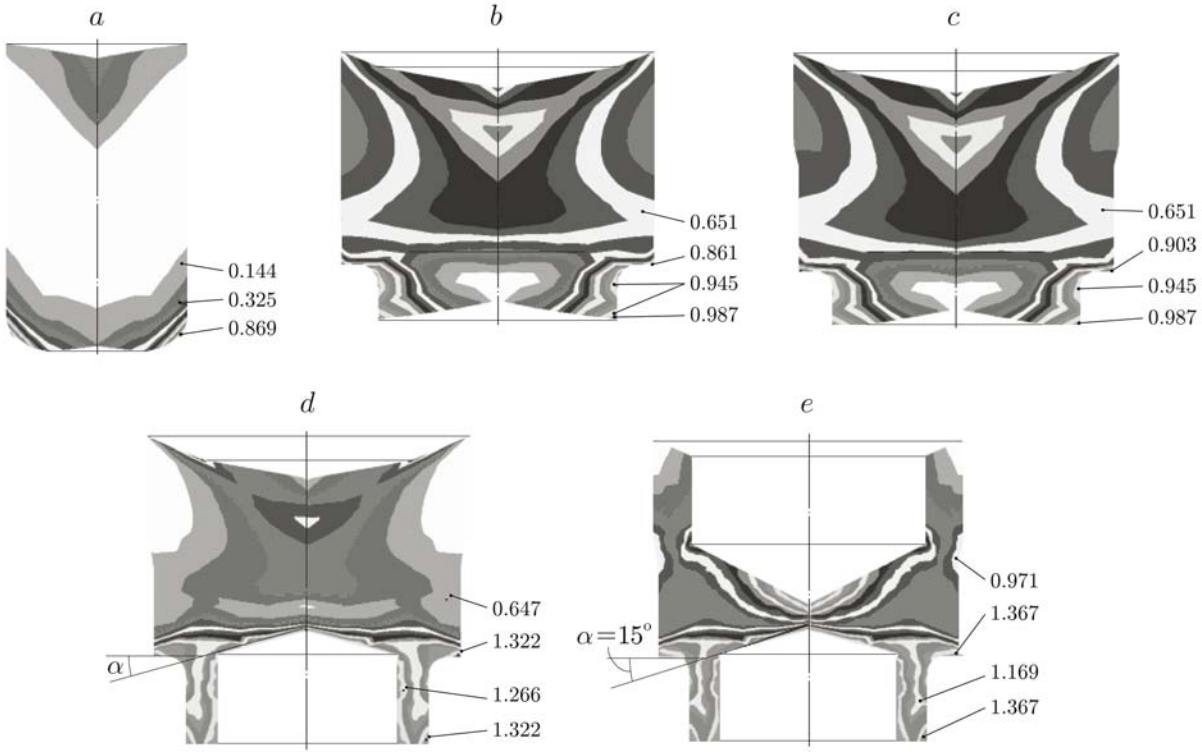

Fig. 7. Accumulated strain intensity field ($\varepsilon = \int d\varepsilon$) in the volume of the blank for $p = 699.3$ (a), 994 (b), 1416 (c), 1466.8 (d), and 1597 MPa (e).

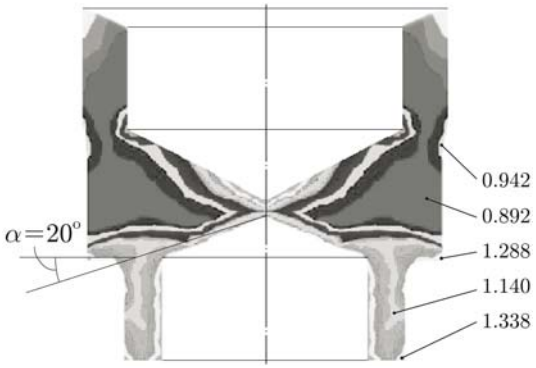

Fig. 8. Accumulated strain intensity fields in the last step using the advanced forging technology ($p = 1498$ MPa).

Friction on the contact surfaces between the blank and extruder and between the die walls and the punch end was described using the Siebel formula $F_{\text{fr}} = \mu\sigma$, where $\mu = 0.12 = \text{const}$.

We determined the accumulated strain intensity fields in the volume of the blank and the specific forging force in the processing steps $p = P/F$ (P is the forging force at the time of complete filling of the cavity of the die block and F is the area of the projection of the blank onto the horizontal plane).

Figure 7 shows the accumulated strain intensity fields and specific forging forces in all five forging steps. It is evident that the strains in the steps reach large values. Even after the second step, the strain intensity is $\varepsilon \geqslant 0.44$ over the entire volume of the blank (Fig. 7b). At the beginning of the last forging step, the strain is somewhat equalized over volume of the blank, and at the end, it is in the range $\varepsilon \in (0.723; 1.367)$ (Fig. 7e).

In cold forging, the admissible load on the tool (punches and dies) is $p < 2000$ MPa. At $p \geqslant 2000$ MPa, the life of the expensive tool decreases sharply. The maximum value $p = 1597$ MPa is observed in the fifth processing step (see Fig. 7e).

The results of tests of this technology lead to the conclusion that, first, the technology is workable because its parameters do not reach the critical values; second, the technology can be improved. An analysis of the flow patterns in the fourth and fifth steps (see Fig. 7d and e) shows that these steps can be combined. In this case, the formation of the upper cavity in the blank by return extrusion will be performed due to the response of the deformation force under which the lower cavity of the blank is formed by direct extrusion, i.e., overlapping of the steps will not lead to an increase in the force necessary for deformation. In addition, this force can be decreased by increasing the angle α from 15 to 20°, which will lead to an increase in the life of die block.

By mathematical modeling of the combined step, it was established that the cavity of the die block is filled without defects (cramps and folds), and the specific forging force decreases from 1597 to 1498 MPa (Fig. 8).

Thus, in the case of complex, in particular, cyclic loading with large strains, the proposed plasticity model more accurately describes the plastic behavior of metals than the classical isotropic and isotropic-translation theories of flow.

REFERENCES

1. G. A. Navrotskii (ed.), *Forming and Forging: Handbook*, Vol. 3: *Cold Forging* [in Russian], Mashinostroenie, Moscow (1987).
2. V. M. Greshnov, A. V. Botkin, A. V. Napalkov, and Yu. A. Lavrinenko, "Mathematical modeling of multistep cold forging based on the physical and mathematical theory of plastic metal working. 1. Calculation of the stress–strain state," *Kuzn.-Shtamp. Proiz., Obrab. Mater. Davl.*, No. 8, 33–37 (2001).
3. A. Yu. Ishlinskii and D. D. Ivlev, *Mathematical Theory of Plasticity* [in Russian], Fizmatlit, Moscow (2001).
4. G. Z. Voyiadjis and R. K. Abu Al-Rub, "Thermodynamic based model for the evolution equation of the backstress in cyclic plasticity," *Int. J. Plasticity*, No. 19, 2121–2147 (2003).
5. H. Czichos, T. Saito, and L. Smith, *Springer Handbook of Materials Measurement Methods*, Springer, Berlin (2007), pp. 95–102.
6. M. C. Araujo, "Non-linear kinematic hardening model for multiaxial cyclic plasticity," Thesis, Teresina (2002).
7. V. M. Greshnov, O. V. Golubev, and A. V. Rtishchev, "New technological scheme of metal forming," *Kuzn.-Shtamp. Proizv.*, No. 2, 8–10 (1997).
8. V. M. Greshnov, "One plasticity model for problems of plastic metal working," *J. Appl. Mech. Tech. Phys.*, **49**, No. 6, 1021–1029 (2008).
9. V. M. Greshnov, Yu. A. Lavrinenko, and A. V. Napalkov, "Engineering physical model of the Bauschinger effect and the governing equations of an isotropic material with anisotropic hardening (tensor relation)," *Kuzn.-Shtamp. Proiz.*, No. 6, 3–6 (1998).